International Journal of Science and Research (IJSR)
ISSN: 2319-7064
SJIF (2022): 7.942

Preparation of Tin Oxide Nanoparticles via Co-Precipitation Method for its Future Applications

Shikha Yadav[1], Shreya[2], Peeyush Phogat[3], Ranjana Jha[4], Sukhvir Singh[5]

[1, 2, 3, 4, 5]Research Lab for Energy Systems, Department of Physics, Netaji Subhas University of Technology, New Delhi, India
Email: *shreyasharma. aug15[at]gmail.com*
[1]0009 - 0001 - 0676 – 3135
[2]0000 - 0002 - 4339 – 1756
[3]0000 - 0002 - 3858 – 6233
[4]0000 - 0003 - 4495 – 3519
[5]0000 - 0003 - 3770 – 0265

Abstract: ***Tin oxide have gained significant attention due to their wide application in optoelectronics, electrodes for lithium - ion batteries, solar cells and gas sensing applications. Owing to its mechanical stability, as well as a high surface - to - volume ratio in comparison to bulk tin oxide, tin oxide (SnO_2) serves as an n - type wide band - gap semiconductor in gas sensing devices. This unique characteristic contributes to enhanced sensitivity and adsorption capabilities. In this study, the chemical co - precipitation method was utilized to synthesize SnO_2 nanoparticles. Among the suggested techniques, the chemical co - precipitation approach has various benefits such as simplicity of use, minimal laboratory equipment requirement, low impurity levels, shorter processing time, and reproducibility. Hence, technique was adopted to synthesis of SnO_2 nanoparticles (NPs). The tetragonal crystal structure of the highly crystalline SnO_2 material was verified by X - ray diffraction (XRD) analysis, revealing a crystallite size of approximately 13 nm using the size - strain plot. Additionally, the absorbance plot and band gap value of the synthesized SnO_2 nanoparticles were determined using UV - Vis spectrophotometer. The morphological features of the as - prepared sample were examined using field emission scanning microscopy (FESEM).***

Keywords: SnO_2, Co - precipitation, band gap, nanoparticles

1. Introduction

Numerous studies on metal oxides, including ZnO, SnO_2, among others have been carried out, to investigate their response to oxidizing and reducing gases [1]. Metal oxides exhibit remarkable promise as fundamental materials in advancing technologies. Recently, extensive research efforts have been dedicated to exploring new applications for these materials, encompassing optical, electronic [2], optoelectronic [3], and biological domains. Tin oxide (SnO_2) stands out as a highly significant n - type oxide, characterized by a broad band gap of 3.6 eV [4]. This semiconductor exhibits excellent electrical, optical, and electrochemical properties of high quality that make it ideal for rechargeable Li batteries and solar cells. [4]. Consequently, there is a growing emphasis on research into this oxide, particularly focusing on preparation methods, as well as its electrical and optical characteristics. The optical characteristics of this material are noteworthy for two primary reasons. Firstly, SnO_2 stands out as one of the few electrical conductors that maintains optical transparency within the visible range of wavelengths in its undoped state [5]. Secondly, it represents the most straightforward oxide semiconductor with a noncubic structure and lacks orbital complexities. Due to these considerations, the optical characteristics of diverse tin oxide materials have undergone thorough and comprehensive study in previous research endeavors. For over four decades, there has been significant interest in semiconducting tin oxide (SnO_2) gas sensors [5], [6]. This interest is attributed to the favorable physical and chemical properties of SnO_2, along with its ability to detect a wide range of gases, including both reducing and oxidizing agents, exhibiting a high response. Presently, global studies are focused on creating cost - effective, compact, and low - maintenance NO_2 gas sensors that demonstrate heightened responsiveness at lower operating temperatures [3], [7]. Since, NO_2 is an oxidizing gas, it is anticipated that a SnO_2 sensor with a significantly lower initial resistance value in air will yield a superior sensing response [8]. Hydrothermal methods [3], chemical vapor deposition [7], the sol–gel method [10], and other techniques have all been developed for the synthesis of SnO_2 nanostructures. The present work employs the chemical co - precipitation technique to synthesize and investigate the properties of SnO_2 nanoparticles.

2. Experimental Section

2.1 Chemicals Used

For synthesis, Tin (II) chloride dihydrate ($SnCl_2.2H_2O$), ethylenediamine ($C_2H_8N_2$) and hydrazine (N_2H_4) was obtained from M/s Fisher Scientific Pvt. Ltd. Tellurium oxide (TeO_2) procured from M/s Sigma Aldrich Pvt. Ltd. was also employed in this study. Ultra - pure water with a resistivity of 5 Mega - Ohms was used for cleansing purposes.

2.2 Synthesis of tin oxide nanoparticles

In the preparation of tin oxide nanoparticles, 0.1 M $SnCl_2.2H_2O$ was dispersed in 40 mL of deionized (DI) water, with the addition of 20 mL of N_2H_4 to this solution. Subsequently, 0.1 M TeO_2 in 40 mL of DI water was dissolved, and 20 mL of $C_2H_8N_2$ was added to it. At room temperature the two solutions were stirred for 30 minutes each. The prepared solutions were then mixed dropwise and stirred for an additional 30 minutes. The resulting solution underwent centrifugation followed by washing using DI water and ethanol three times. Thereafter, it was kept in a vacuum oven maintained at 60˚C for the duration of 24 hours, resulting in the formation of dark grey colored powdered material.

3. Results and Discussion

3.1 Characterization Details

The prepared sample was subjected to analysis using a Panalytical model X'pert PRO X - Ray Diffractometer. Cu Kα radiation (=1.5406 Å) was used to record the X - ray diffraction pattern. A FESEM (model: 7610FPlus, make: JEOL) was used for morphological analysis. Using a SHIMADZU UV - 2600i UV - Vis spectrophotometer the optical response was recorded.

3.2 X - Ray Diffraction

The prepared sample's XRD pattern was captured at 2θ values between 10° and 80°. The analysis indicates the formation of tin oxide nanoparticles as matched with JCPDS file no. (01 - 077 - 0451). The characteristic peaks of (110), (101), (200), (211), (220), (310), (301) also matched with JCPDS file no. (01 - 077 - 0451) indicating the tetragonal crystal structure formation. The diffraction peaks shown in fig.1. (a) corresponded to the crystal structure of SnO_2, exhibiting a space group of P42/mnm and a space number as 136. The presence of several sharp peaks resembles the formation of highly crystalline material with crystallinity of 87%. Using the space group and space number information, a three - dimensional model illustrating the tetragonal crystal system of SnO_2 has been included in fig.1.

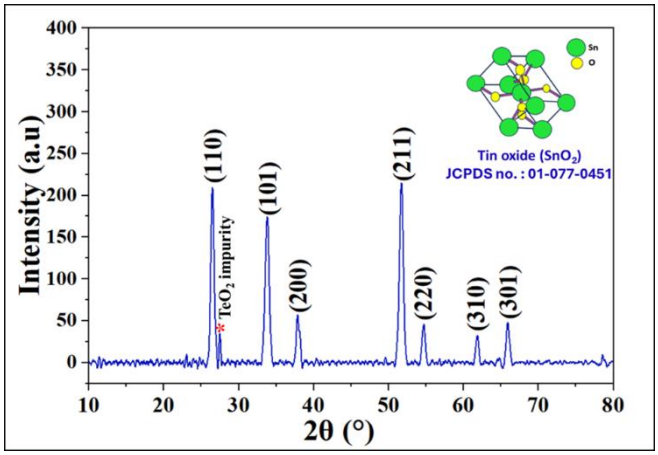

Figure 1: XRD pattern along with crystal structure of SnO_2.

Lattice Parameters, Crystallite Size and Strain. The lattice parameter is a fundamental step in understanding the crystallographic and structural characteristics of the as - prepared sample. The lattice parameters value was calculated using equation (1) [11],

$$\frac{1}{d} = \frac{h^2+k^2}{a^2} + \frac{l^2}{c^2} \text{ for tetragonal } SnO_2 \qquad (1)$$

In equation (1), a, b, c means lattice parameter; (h, k, l) denotes the miller indices; and d indicates interplanar spacing. The evaluated values of lattice parameter mentioned in table 1 shows some variations from the standard value, attributed to the presence of TeO_2 impurities in the prepared sample.

The Debye - Scherrer equation was employed for determining the crystallite size of the as - synthesized SnO_2 particles as given in equation (2) [12],

$$D = \frac{k\lambda}{\beta \cos\theta} \qquad (2)$$

where, k denotes the Scherrer constant (k=0.9), λ represent X - ray wavelength (λ=1.54 Å), β indicates the full width at half maximum (FWHM) of the peak, θ indicates the peak position, and D is defined as size of crystallite. Equation above was used to determine the crystallite size of as - prepared tetragonal SnO_2. The obtained crystallite size was found to be approx.25 nm. At this scale, the material may exhibit unique properties compared to bulk counterparts due to increased surface - to - volume ratios [13]. The crystallite size determined through the Debye - Scherrer equation has limited accuracy, as this method assumes an ideal scenario of defect - free crystallites. Williamson - Hall (W - H) plot considers both crystallite size and lattice strain effects, providing a more comprehensive analysis of the sample using equation (3) [14],

$$\beta_T \, Cos\Theta = (\varepsilon \times 4Sin\Theta) + \frac{K\lambda}{D} \qquad (3)$$

The W - H plot was generated by plotting $\beta\cos\theta$ on the vertical axis against $4\sin\theta$ on the horizontal axis. The gradient of this plot corresponds to the strain within the as - prepared sample while the intercept is utilized to determine the crystallite size value using the equation (4) [12],

$$D = \frac{k\lambda}{Intercept} \qquad (4)$$

The obtained values of crystallite size and lattice strain via W - H plot are mentioned in table 2. The positive value of strain reveals the presence of tensile strain [15]. However, strain determined from the W - H plot is expressed in microstrain, and the calculated crystallite size is based on the irregular FWHM values. To get more accurate value of crystallite size and lattice strain, the S - S (size - strain) plot was employed in which the normalized FWHM values which were obtained by rietveld analysis were used. The presence of strain and value of crystallite size in the as - prepared sample were found using the equation (5) [16],

$$(d_{hkl} \times \beta_{hkl} \times Cos\Theta)^2 = \frac{K\lambda}{t} \times (d^2_{hkl} \times \beta_{hkl} \times Cos\Theta) + \frac{\varepsilon^2}{4} \qquad (5)$$

The S - S plot was used because it calculates strain more accurately than the W - H plot, which considers strain in all directions when analyzing crystallite size and strain in materials, and the Debye - Scherrer method, which assumes no defects in the crystallite structure. The values for crystallite size and lattice strain derived through Debye - Scherer equation, W - H and S - S plot are presented in the table 2.

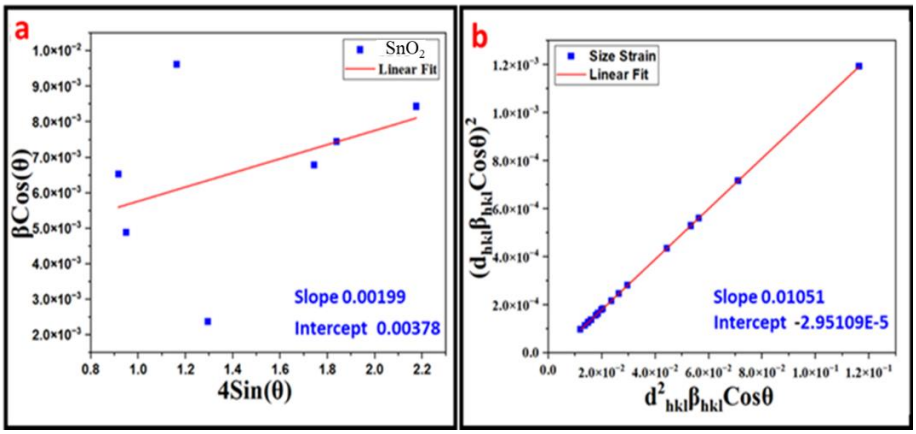

Figure 2: (a & b) W - H plot and S - S plot of the as - prepared SnO_2

Table 1: Lattice Parameters of the as - prepared SnO_2 corresponding to JCPDS data.

Crystallographic Parameter	JCPDS Value	Evaluated value
a (Å)	4.75	4.75
b (Å)	4.75	4.75
c (Å)	3.19	1.58

Table 2: Value of Crystallite size and lattice strain in the as - prepared SnO_2.

Method Used	Size of Crystallite	Strain
Debye - Scherrer	25 nm	-
W - H plot	36 nm	0.00199
S - S plot	13 nm	0.01089

3.3 UV - Vis Spectroscopy

UV - visible spectroscopy was used to analyse the optical properties of the SnO_2 sample in its prepared state between 190 and 850 nm in wavelength.

The graph exhibits multiple peaks, with the highest absorbance observed in the ultravi - olet region and no absorption detected in the visible region. The absorbance curve plotted in the fig.3. (a) shows that maximum absorbance at 193 nm which indicates strong interactions between the material and incident light in the ultraviolet spectrum. The absorption peaks depicted in fig.3. (a) are 193, 227.5, 259.5, 273, 286, and 373.5 nm. Using the absorbance data, the Tauc plot was calculated by applying Beer Lambert's law as given in equation (6) [12], [16] to find the energy band gap of the as - prepared SnO_2 through linear fitting of the data.

$$\alpha h\nu = A\,[h\nu - E_g]^{1/n} \quad (6)$$

where, α indicates Sample's absorption coefficient, h is Planck constant, $\boldsymbol{\nu}$ =λ (wavelength) /c (speed of light). For materials with a direct band gap, the value of n is ½, whereas for those with an indirect band gap, it is 2. The Tauc's plot for the as - prepared sample was calculated by linear fitting the specific region, the band gap was found to be 3.4 eV. Prior studies have indicated a band gap of approximately 3.6 eV [3], [9], indicating a modest decrease in the band gap value of the produced sample. However, the prepared sample can be utilized in gas sensor technology due to its large band gap [17], [18]. Its high sensitivity to certain gases, such as carbon monoxide (CO) and methane (CH_4), makes it valuable for detecting gas leaks and ensuring safety in various industries.

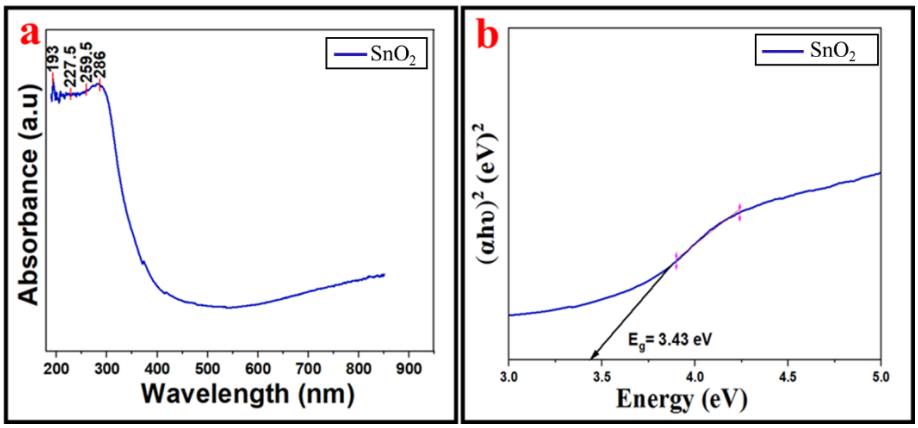

Figure 3: (a) Absorbance plot of as - prepared SnO_2 & **(b)** Tauc's plot of as - prepared SnO_2

Refractive index and HOMO & LUMO levels. In the design and fabrication of photonic devices, the refractive index is essential for determining the behavior of light within the device and can also influence sensor sensitivity [6], [11]. It was calculated using equation (7) [16], [12],

$$\frac{n^2-1}{n^2+2} = 1 - \sqrt{\frac{E_g}{20}} \quad (7)$$

where, E_g refers to the energy band gap. The value calculated for the as - prepared sample was 2.2, closely aligning with the standard range of 1.9 to 2.1. The HOMO and LUMO energy levels were found using equation (8) and (9) [19],

$$E_{VB} = \chi — E_e + 0.5\, E_g \quad (8)$$
$$E_{CB} = E_{VB} + E_g \quad (9)$$

E_{VB} is the energy level associated with the valence band, also known as the Highest Occupied Molecular Orbital (HOMO), χ represents the absolute electronegativity of the material, E_e denotes the free electron energy, referenced on the hydrogen scale with a standard value of 4.5. E_g represents the optical band gap, representing the energy difference between the Valence Band and the Conduction Band. E_{CB} corresponds to the energy level of the Conduction Band, also referred to as the Lowest Unoccupied Molecular Orbital (LUMO). The relationships between these parameters are essential for understanding the electronic structure and energy levels in a material. The obtained value of HOMO level and LUMO level found using as - calculated value of band - gap is 3.45 eV and 6.88 eV respectively. Materials with the HOMO level value near to the band gap are of interest in photovoltaic applications, as they may facilitate efficient charge separation.

3.4 Field Emission Scanning Electron Microscopy (FESEM)

The morphology of the as - synthesized sample was examined at various magnifications. Nanoparticles with polyhedral shaped morphology are formed on the surface confirming the formation of SnO_2 particles as shown in the Fig.4 (a & b). The agglomerated image of a polyhedral nanostructure is shown in images below. These images were captured at different areas, utilizing a suitable range of magnification, spanning from 100 nm to 1µm. The comprehensive analysis provided valuable insights into the uniformity and structure of the nanoparticles, enriching our understanding of the sample's characteristics.

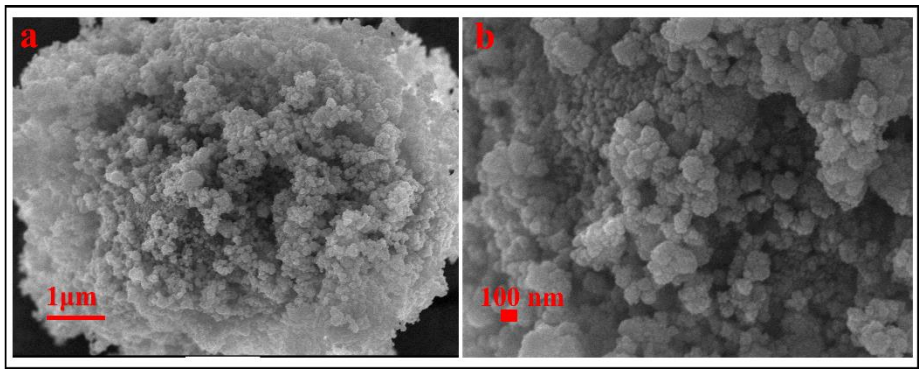

Figure 4: (a) & (b) FESEM images of as - prepared SnO_2.

4. Conclusion

In this study the tin oxide nanoparticles were prepared using co - precipitation method for their future applications. Characterization techniques such as XRD, UV - Vis spectrophotometer, and FESEM were used to investigate the properties of the material.

XRD data was analyzed which confirmed the highly crystalline structure of the as - prepared sample holding a crystallinity of 87%. The diffraction pattern revealed the presence of tin (IV) oxide with some impurity of TeO_2. The average crystallite size was determined to be 25 nm using the Scherrer equation, 36 nm with the W - H plot, and 13 nm using the S - S plot. The lattice strain observed in the as - prepared sample 0.00199 and 0.01089 as calculated by W - H and S - S plots, respectively. The tauc plot was generated through analysis of the absorbance graph, revealing a bandgap value of 3.4. The obtained bandgap showed little deviation from the standard value i. e.3.6 due to presence of TeO_2 impurities and some amorphous content in the as - prepared sample. The calculated value of refractive index was 2.2. Additionally, the calculated valence band value was 3.45 eV and the value of conduction band was 6.88 eV, based on the bandgap. Furthermore, the characterization of SnO_2 through FE - SEM images revealed the formation of polyhedral shaped nanoparticles. In this study, the nanoparticles were synthesized without the need for a specialized atmosphere or high - pressure conditions. This study outlines a straightforward and dependable method for the preparation of tin oxide, indicating its extensive potential for future applications.

Acknowledgements
The authors sincerely appreciate the support and resources provided by Prof. Anand Srivastava, Vice Chancellor of Netaji Subhas University of Technology (formerly Netaji Subhas Institute of Technology, University of Delhi).

Author contributions
Shikha Yadav: Conceptualization, Writing - original draft and Formal analysis. Shreya: Formal analysis and software. Peeyush: Formal analysis and software. Sukhvir Singh: Writing - review & editing. Ranjana Jha: Supervision.

References

[1] Feng, Z. H. Ge, Y. X. Chen, J. Li, and J. He, "Hydrothermal synthesis of SnQ (Q = Te, Se, S) and their thermoelectric properties, " *Nanotechnology*, vol.28, no.45, p.455707, Oct.2017, doi: 10.1088/1361 - 6528/AA8B29.
[2] H. Hashtroudi, "Two - Dimensional Materials for Hydrogen Gas Sensing Applications. "
[3] S. Das and V. Jayaraman, "SnO2: A comprehensive review on structures and gas sensors, " *Progress in Materials Science*, vol.66. Elsevier Ltd, pp.112–255, 2014. doi: 10.1016/j. pmatsci.2014.06.003.
[4] W. Chen, Q. Zhou, F. Wan, and T. Gao, "Gas sensing properties and mechanism of Nano - SnO2 - based sensor for hydrogen and carbon monoxide, " *J Nanomater*, vol.2012, 2012, doi: 10.1155/2012/612420.
[5] Q. - H. Wu, J. Li, and S. - G. Sun, "Nano SnO 2 Gas Sensors, " 2010.

[6] W. Chen, Q. Zhou, F. Wan, and T. Gao, "Gas sensing properties and mechanism of Nano - SnO2 - based sensor for hydrogen and carbon monoxide, " *J Nanomater*, vol.2012, 2012, doi: 10.1155/2012/612420.
[7] Y. J. Choi, I. S. Hwang, J. G. Park, K. J. Choi, J. H. Park, and J. H. Lee, "Novel fabrication of an SnO2 nanowire gas sensor with high sensitivity, " *Nanotechnology*, vol.19, no.9, Feb.2008, doi: 10.1088/0957 - 4484/19/9/095508.
[8] A. Di6guez, A. Romano - Rodriguez, J. R. Morante, U. Weimar, M. Schweizer - Berberich, and W. G6pel, "Morphological analysis of nanocrystalline SnO2 for gas sensor applications, " 1996.
[9] Y. J. Choi, I. S. Hwang, J. G. Park, K. J. Choi, J. H. Park, and J. H. Lee, "Novel fabrication of an SnO2 nanowire gas sensor with high sensitivity, " *Nanotechnology*, vol.19, no.9, Feb.2008, doi: 10.1088/0957 - 4484/19/9/095508.
[10] W. Chen, Q. Zhou, F. Wan, and T. Gao, "Gas sensing properties and mechanism of Nano - SnO2 - based sensor for hydrogen and carbon monoxide, " *J Nanomater*, vol.2012, 2012, doi: 10.1155/2012/612420.
[11] P. PHOGAT,. S., R. JHA, and S. Singh, "Electrochemical Analysis of Thermally Treated Two Dimensional Zinc Sulphide Hexagonal Nano - Sheets with Reduced Band Gap, " *Phys Scr*, Dec.2023, doi: 10.1088/1402 - 4896/ad0d93.
[12] P. Phogat, Shreya, R. Jha, and S. Singh, "Optical and Microstructural Study of Wide Band Gap ZnO[at]ZnS Core–Shell Nanorods to be Used as Solar Cell Applications, " pp.419–429, 2023, doi: 10.1007/978 - 981 - 99 - 2349 - 6_38/COVER.
[13] S. Tazikeh, A. Akbari, A. Talebi, and E. Talebi, "Synthesis and characterization of tin oxide nanoparticles via the Co - precipitation method, " *Materials Science - Poland*, vol.32, no.1, pp.98–101, 2014, doi: 10.2478/s13536 - 013 - 0164 - y.
[14] Shreya, P. Phogat, R. Jha, and S. Singh, "Microwave - synthesized γ - WO3 nanorods exhibiting high current density and diffusion characteristics, " *Transition Metal Chemistry*, vol.48, no.3, pp.167–183, Jun.2023, doi: 10.1007/S11243 - 023 - 00533 - Y.
[15] B. Bharti, P. B. Barman, and R. Kumar, "XRD analysis of undoped and Fe doped TiO2 nanoparticles by Williamson Hall method, " in *AIP Conference Proceedings*, American Institute of Physics Inc., Aug.2015. doi: 10.1063/1.4929241.
[16] T. Kumar, Shreya, P. Phogat, V. Sahgal, and R. Jha, "Surfactant - mediated modulation of morphology and charge transfer dynamics in tungsten oxide nanoparticles," *Phys Scr*, vol.98, no.8, Aug.2023, doi: 10.1088/1402 - 4896/ACE566.
[17] A. Di6guez, A. Romano - Rodriguez, J. R. Morante, U. Weimar, M. Schweizer - Berberich, and W. G6pel, "Morphological analysis of nanocrystalline SnO2 for gas sensor applications," 1996.
[18] Q. - H. Wu, J. Li, and S. - G. Sun, "Nano SnO 2 Gas Sensors," 2010.
[19] Dipti, P. Phogat, Shreya, D. Kumari, and S. Singh, "Fabrication of tunable band gap carbon based zinc nanocomposites for enhanced capacitive behaviour, " *Phys Scr*, vol.98, no.9, Sep.2023, doi: 10.1088/1402 - 4896/ACF07B.